PNAS
www.pnas.org

http://www.pnas.org/page/authors/submission#preparation

Supplementary Information for:

Critical symbiont signals drive both local and systemic changes in diel and developmental host gene expression

Silvia Moriano-Gutierrez, Eric J. Koch, Hailey Bussan, Kymberleigh Romano, Mahdi Belcaid, Federico E. Rey, Edward Ruby, and Margaret McFall-Ngai

Margaret McFall-Ngai
Email: mcfallng@hawaii.edu

This PDF file includes:

- Supplementary text
- Figs. S1 to S10
- Tables S1 to S3
- Captions for movies S1 to S3
- Captions for databases S1 to S10
- References for SI reference citations

Other supplementary materials for this manuscript include the following:

- Movies S1 to S3
- Datasets S1 to S10

www.pnas.org/cgi/doi/10.1073/pnas.1819897116

Supplementary Information Text

SI Results

Sequencing, Assembly and Annotation. We sequenced total RNA isolated from 45 samples across 3 distinct tissue types and two developmental stages. The 2.2 billion paired-end reads were de novo assembled, yielding 788,971 contigs (Fig. S1 and Dataset S1). Ninety percent of the expression was represented by only 16,295 transcripts, and 70% of all transcripts with an open reading frame had BLASTx annotations, which had highest representation within closely related taxa (Fig. S1*C* and *D*). For all three squid organs considered together, the 'biological process' category constituted the highest percentage (47%) of Gene Ontology (GO) mapping of the transcripts, followed by 'cellular component' (35%) and 'molecular function' (18%) (Fig. S1*E*).

SI Materials and Methods

General Procedures. Adult *Euprymna scolopes* squid were collected from Paikō Lagoon, Oahu, Hawai'i, and either transferred to outdoor tanks to maintain natural light cues or transported to the University of Wisconsin (Madison, WI) and maintained in the laboratory as previously described (1). Juveniles from the breeding colony were collected within minutes of hatching, and placed in either filter-sterilized Instant Ocean (FSIO) artificial seawater (Aquarium Systems, Mentor, OH) or filter-sterilized coastal ocean water. Within 2 h of hatching, juveniles were either made symbiotic (SYM) by overnight exposure to cells of *Vibrio fischeri* in filter-sterilized ocean water (FSIO), or kept aposymbiotic (APO) (2). For all experiments, animals were maintained on a 12-h light-dark cycle and, when needed, squid males were raised for 5-6 months to adulthood, following standard procedures (3). All of the adult squid used, including both, reared or wild-caught, were males, and had mantle lengths between 2.51 and 2.82 cm, indicating that they were fully mature.

Two strains of *V. fischeri* were used in this study: the wild-type ES114 (2) and its dark-mutant derivative EVS102 (Δ*lux*), in which the genes required for luminescence were deleted (4). To prepare the strains as an inoculum, they were first cultured overnight in Luria-Bertani salt medium (LBS) (5). They were then subcultured (1:100) into seawater tryptone medium (SWT) (2), and grown to mid-log phase at 28 °C with shaking. This subculture was diluted into seawater to a final concentration of 3,000-5,000 cells/ml, and juvenile squid added. Colonization of the host was monitored by checking for animal luminescence with a TD 20/20 luminometer (Turner Designs, Sunnyvale, CA) or, in

animals colonized by EVS102, by plating the surrounding water after the dawn expulsion. Juvenile animals were collected at the indicated times after inoculation, anesthetized in seawater containing 2% ethanol, and stored frozen at -80 °C in RNAlater (Ambion), as previously described (6), until further processing.

Host Organ RNA Extraction and Sequencing. Total RNA was purified using QIAGEN RNeasy columns, immediately followed by treatment with TURBO™ DNase (Ambion). The RNA concentration for each sample was then determined with a Qubit RNA BR assay kit (Invitrogen). The Illumina TruSeq protocol v2.0, with polyA selection, was used throughout to generate bar-coded sequencing libraries for all 24 h samples. Paired-end 100-bp sequencing was performed at the University of Wisconsin-Madison Biotechnology and Gene Expression Center. The Illumina TruSeq Stranded mRNA Sample Prep with polyA selection v4.0 protocol was used for all adult samples of light organ and gill tissues (at the University of Utah High-Throughput Genomics Core Facility) and for eye tissues (at SeqMatic, Fremont, CA. All sequencing data was used to build the reference transcriptome (see below).

De Novo RNA-Seq Assembly and Annotation. Trimmomatic (7), was used to trim and discard reads containing the Illumina adaptor sequences with a minimum length threshold of 36 bp. A total of 2.2 billion paired-end reads were *de novo* assembled into the Trinity-v2.4.0 RNA-Seq assembler (8) incorporating an *in silico* normalization step (Dataset S1). A BLASTx search against the NCBI non-redundant protein database was used to annotate the reference transcriptome. For the functional annotations of the reference transcriptome, Gene Ontology (GO) mapping of the transcripts and gene set enrichment analysis (GSEA) (9) as performed with Blast2go software (10).

Transcript Abundance Estimation and Differential Expression Analysis. Reads were mapped against the reference transcriptome with bowtie2 (11), and their relative expression values for each tissue were estimated with RSEM software (12). The statistical analysis of the RNA-Seq data was performed with the R package edgeR (13), identifying the significantly differentially expressed transcripts in each of the pairwise comparisons, and employing a false discovery rate (FDR) threshold of 0.05 with at least a 2-fold change in expression difference. However, when we determined the sets of tissue-specific genes, the cut off for fold-change difference was set to 8-fold. Only genes with expression values

of >0.5 FPKM (fragments per kilobase of transcript per million fragments mapped) in at least 2 samples of the pairwise comparisons were included in the analysis. The count data of the remaining genes were normalized and log-transformed in edgeR. All normalized mean expression values are shown in Dataset S2**.** All normalized expression values were used to determine the threshold of expression for all tissues, where a gene is considered expressed if it has an expression value equal to or larger than 0.5 FPKM in all samples of that tissue. Due to the large differences in expression profiles of the different tissues at both developmental stages, the determination of expressed genes per tissue was performed separately for juvenile and adult samples. Venn diagrams were drawn using the venn function of ggplot R package. Heatmaps of expression values and hierarchical clustering were created with heatmap3 and hclust functions, respectively, in the R environment (14). Statistical enrichment of Gene Ontology (GO) terms for differentially expressed genes was performed in Blast2Go software (10) using the Fisher exact test with an FDR<0.01. In addition, gene-set weighted enrichment analysis (GSEA) with 500 permutations and FDR < 0.1 was performed on the differentially expressed transcripts (Dataset S10). No significant difference was seen for the top enriched terms between the two methods.

Quantitative NanoString nCounter Analysis and Gene Transcript Quantification by qPCR. The nCounter Custom CodeSet (Dataset S3) Kit (NanoString Technologies) was used to detect changes in gene expression following the manufacturer's protocol. Total RNA, was extracted as described above. Assay and spike-in controls were used for normalization based on identical amounts of input RNA. Welch's t-test analysis was performed with nSolverAnalysis Software v3.0. Ribosomal protein 19L, serine hydroxymethyl transferase and peptidyl-prolyl cis-trans isomerase were used as internal reference genes to normalize expression levels of each candidate gene, using their geometric means (15). Pearson correlation of expression data obtained by RNA-Seq and NanoString was calculated with GraphPad Prism v7.00 software. Host gene expression changes were in addition measured by qPCR using LightCycler® 480 SYBR Green I Master Mix (Roche). Total RNA, was extracted as described previously. Synthesis of the single-stranded complementary DNA was performed with SMART MMLV Reverse Transcriptase (Clontech) using Oligo(dT)12–18 primers (Invitrogen). All reactions were performed with no-RT and no-template controls to confirm that the reaction mixtures were not contaminated. Specific primers (Table S1) were designed with Primer3plus (16).

Primer efficiencies ranged between 98% and 105% with an annealing temperature of 60 °C for all primer pairs. The amplification efficiency was determined by in-run standard curves with a 10-fold dilution template. Each reaction was done in duplicate with a starting level of 12.5 ng cDNA. The generation of specific PCR products was confirmed by melting-curve analysis. Expression analyses of candidate genes were normalized to the geometric mean of the expression levels of three reference genes: ribosomal protein 19L, serine hydroxymethyl transferase and heat-shock protein 90. Analyses were performed with the MCMC.qpcr R package (17) using an *informed* MCMC qpcr model. Results are reported as $\log_2$ fold-changes with *p*-values calculated using the posterior distribution and corrected for multiple testing. Bar graphs of expression values were produced with GraphPad Prism v7.00 software.

Experimental Procedures with Mice. All experiments involving mice were performed using protocols approved by the University of Wisconsin - Madison Animal Care and Use Committee. C57BL/6 mice were maintained in a controlled environment in plastic flexible-film gnotobiotic isolators [germ-free (GF) mice] or filter-top cages [conventionally raised (CONVR) mice] under a strict 12:12 light:dark cycle, and received sterilized water and food *ad libitum*. The sterility of germ-free animals was assessed by incubating freshly collected fecal samples under aerobic and anaerobic conditions using standard microbiology methods. In total, six 8-week-old female mice, three GF and three CONVR, had both left and right eyes collected 5 h after facility lights were turned on. Animals were euthanized by cervical dislocation and were non-fasted at the time of sacrifice. Collected tissue was preserved in RNAlater, left overnight at 4 ^{o}C, and shipped frozen to the University of Hawaii at Manoa, where samples were kept at -80 ^{o}C until further processing.

RNA Extraction from Mouse Eyes. Total RNA from eye tissue was purified with RNeasy Fibrous Tissue Mini Kit (QIAGEN), immediately followed by treatment with TURBO™ DNase (Ambion) and quantified with Qubit RNA BR assay kit (Invitrogen). The Illumina TruSeq protocol v4.0, TruSeq Stranded RNA kit with Ribo-Zero Gold with polyA selection was done. Sequencing was performed with HiSeq 125 Cycle Paired-End sequencing V4 (New York University, Genome Technology center). Sequencing reads were trimmed and cleaned of adapters with Trimmomatic (7) and then mapped to the mouse genome. Then gene annotations (mm_ref_GRCm38.p4) were derived using TopHat v2.013 (18) with default settings for paired-end samples. Samtools (19) was used to index and sort the

alignments and FeatureCounts (20) in paired-end (-p) exon mode to assign their gene annotations. To identify differentially expressed transcripts the R package edgeR (13) was implemented with a threshold of FDR<0.05 and 2-fold change difference in expression.

Whole-mount Hybridization Chain Reaction, Fluorescence in Situ Hybridization (HCR-FISH) to Detect the Transcript of Atrial Natriuretic-Converting Enzyme. HCR-FISH probes (version3) specific for the host atrial natriuretic-converting enzyme and *V. fischeri* 16S RNA (Table S2) were designed and provided by Molecular Instruments (www.molecularinstruments.org). Juvenile squid were collected 24 h post-colonization under standard procedures explained previously, with the following modifications. After anesthetization with 2% ethanol in seawater, squid were fixed overnight in 4% paraformaldehyde in marine phosphate-buffered saline (mPBS) (3) at 4 °C. The light organs were then dissected out and the hybridization procedure was followed as described in (21), with the following modifications. Probe hybridization was conducted at 37 °C in 30% DNA hybridization buffer (version3; Molecular Instruments). Probe wash buffer (version 3) was used to remove nonspecifically bound probe as specified earlier (21). Samples were counterstained with TO-PRO-3 (Thermo Fisher Scientific) to label host nuclei, and imaged using a Zeiss LSM 710 confocal microscope. Z-stack images of 1024 x 1024 pixels were acquired at acquisition speed 7, with an averaging of 4 images. Fluorescence intensity for all sections of each Z-stack was measured using FIJI (22). The brightness of the final images was adjusted for visual clarity using IMARIS bitplane software.

ACCESSION NUMBERS

The data have been deposited with links to BioProject accession numbers PRJNA473394, PRJNA498343, and PRJNA498345 in the NCBI BioProject database (https://www.ncbi.nlm.nih.gov/bioproject/).

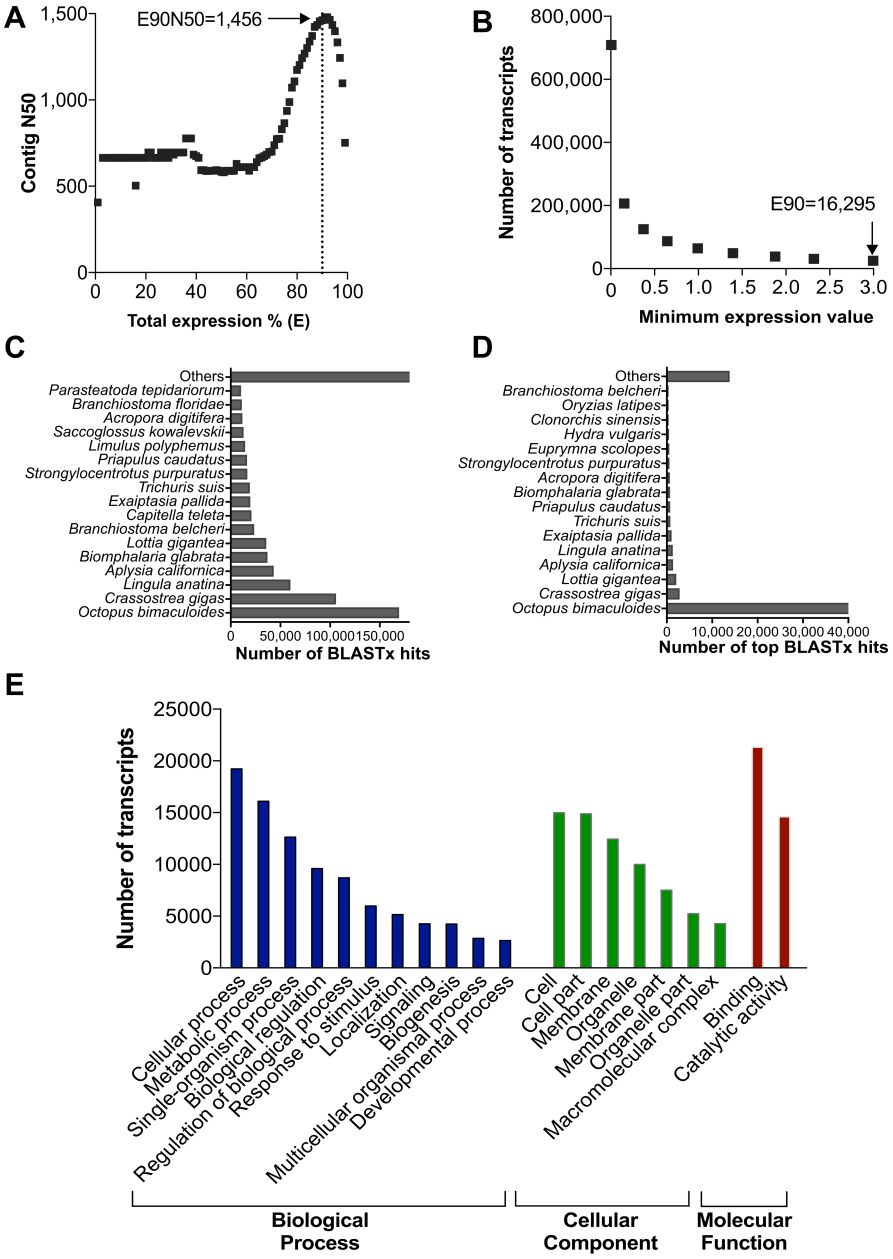

Fig. S1. Assessment of the assembly quality and read representation of the *E. scolopes* transcriptome and its annotation. A. The N50 contig value is calculated from the cumulative sets of the top most highly expressed transcripts that represent the total TMM (Trimmed Mean of M-values)-normalized expression data. E90N50 = 1,456. **B.** The number of most highly expressed transcripts is plotted against the minimum expression value. Ninety percent of the total transcriptional activity is represented by a set of 16,295 transcripts. The expression value is measured as fragments per kilobase million reads (FPKM). **C**. BLASTx species distribution for all blast hits for the squid transcriptome. **D**. Species distribution of blast hits for all top-hit species for the squid transcriptome. To identify homologous genes, the squid transcripts were compared (using BLASTx) against the non-redundant protein database (nr). The E-value cut-off was set at 1.0 E^{-3}. **E.** Functional annotation of *E. scolopes* transcriptome at the 2nd-level GO terms (Dataset S1).

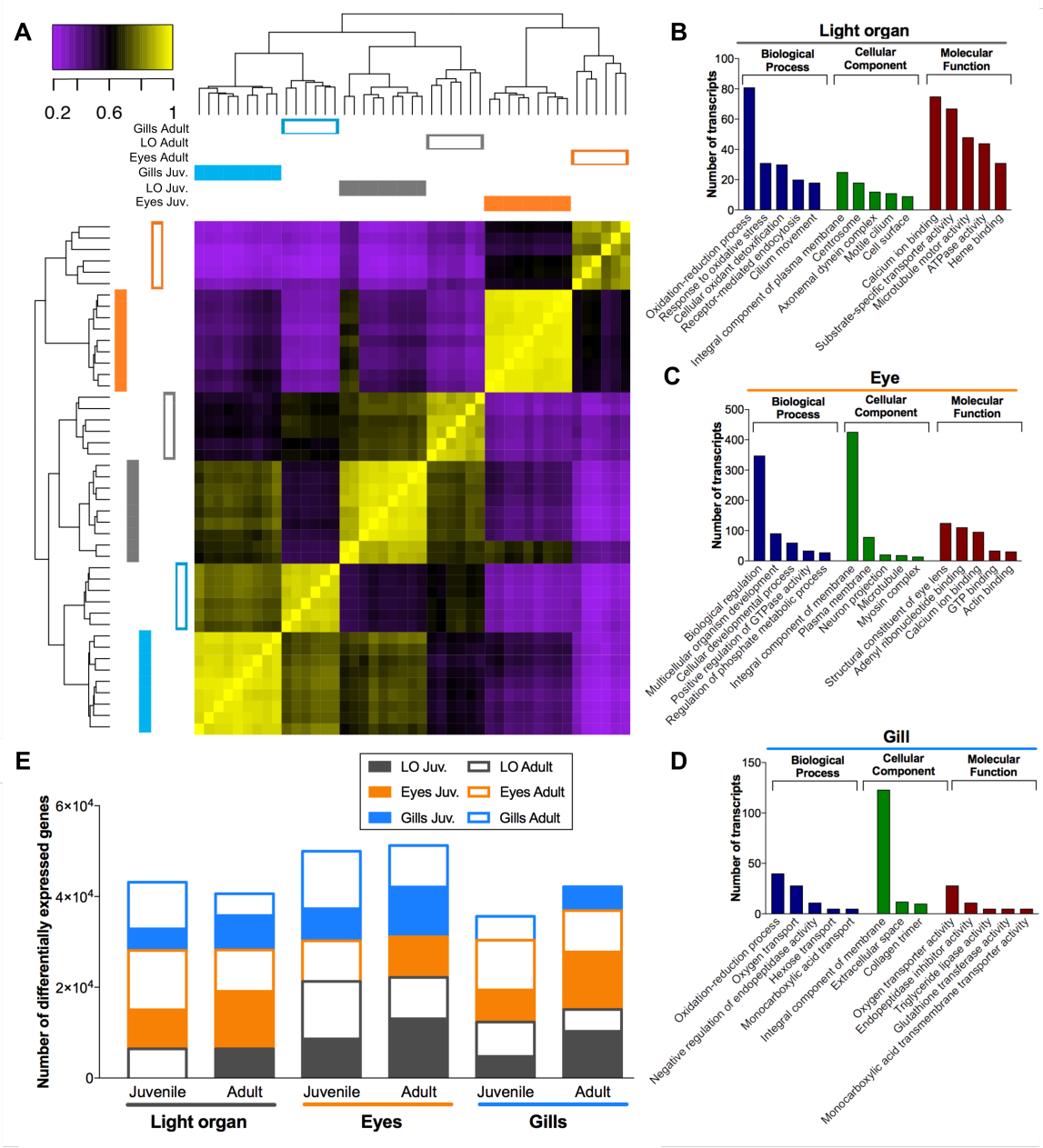

Fig. S2. Data analysis of differentially expressed transcripts across each set of organs, identifying transcripts enriched in specific organs (P_{adj} < 0.05, fold-change > 8). **A**. Hierarchically clustered heatmap based on 21,013 differentially expressed genes, visualizing a correlation matrix of the reference transcriptome. **B-D**. Top 5 GO term enrichment for each category. GO enrichment (p < 0.01 FDR corrected) for differentially expressed genes in **B.** Light organ, **C.** Eyes and **D.** Gills. **E.** The number of differentially expressed genes in each of the five pairwise comparisons between the three analyzed organs, for each of two developmental stages (P_{adj} < 0.05, fold-change > 8). LO= light organ, Juv= 24-h. (Datasets S2 and S3).

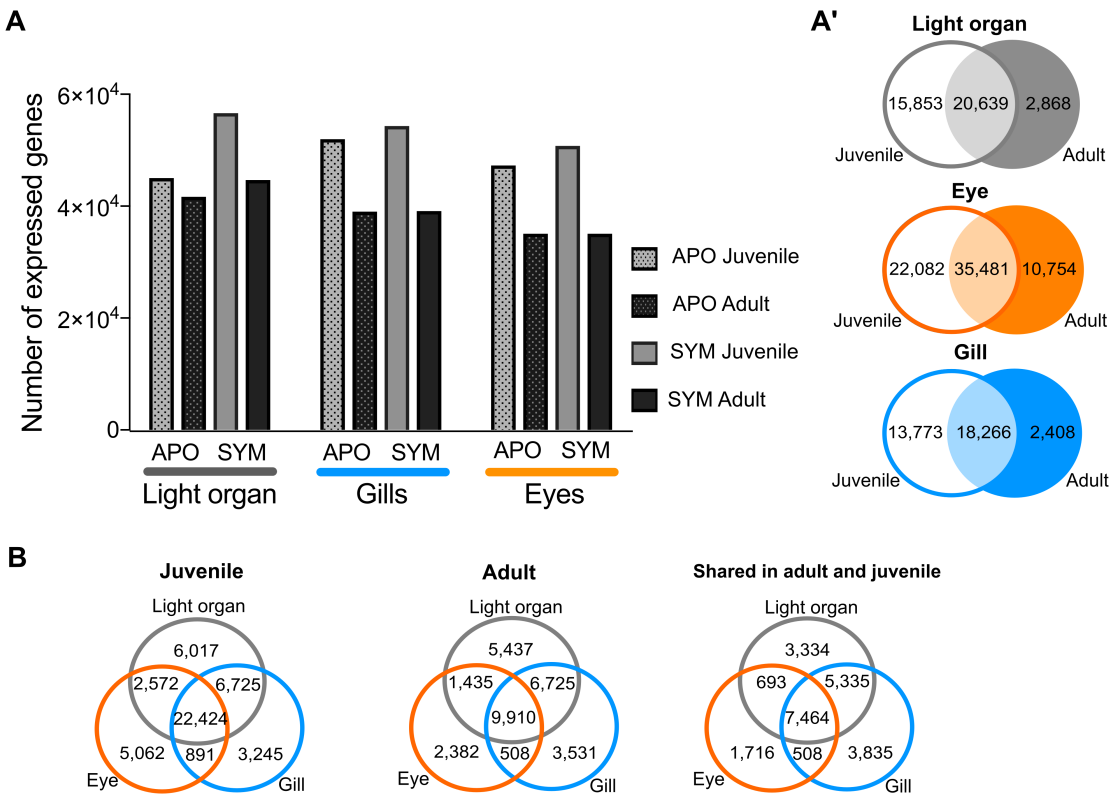

Fig. S3. Symbiosis-responsive genes shared across squid organs and stages of development. A. Summary of distribution of gene abundance across two developmental stages (juvenile and adult) in aposymbiotic (APO) and symbiotic (SYM) individuals. **A'**. Venn diagrams of expressed genes shared between juveniles and adults in each organ. A gene is considered expressed when FPKM > 0.5 in at least two samples. **B.** Venn diagrams of shared expressed genes when FPKM > 0.5 in all samples within the comparison. (Dataset S1).

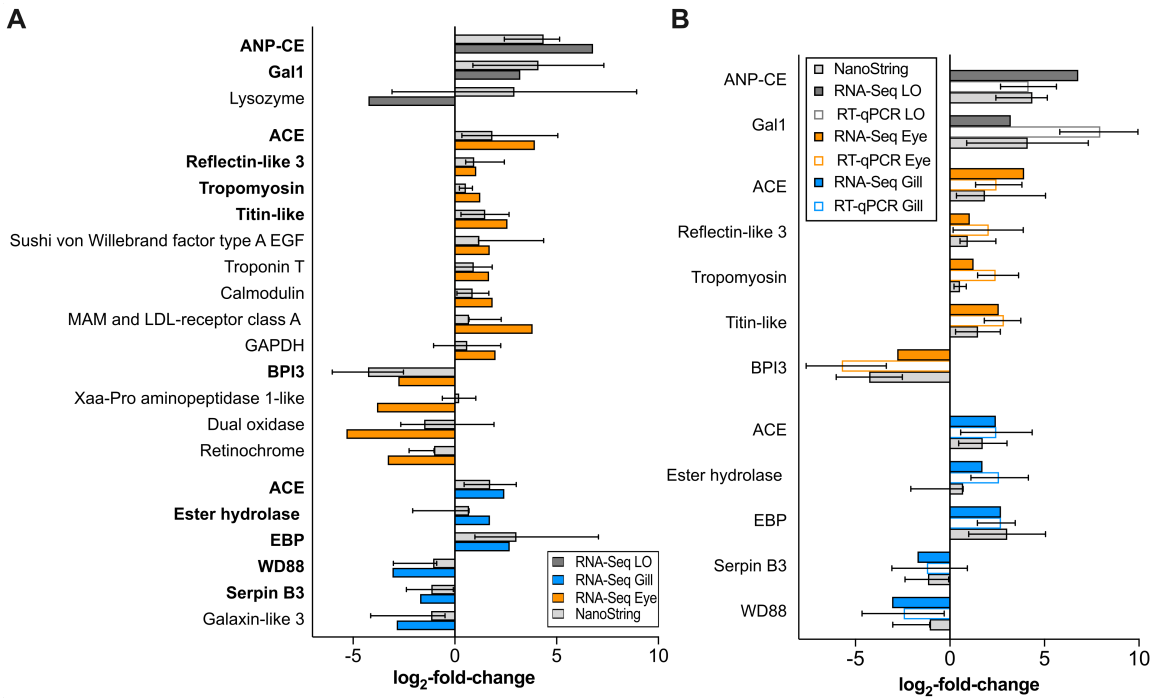

Fig. S4. Validation of adult RNA-seq data by NanoString Technologies. A. The log_2-fold change values determined by NanoString Technologies validated 21 of the set of 22 differentially expressed genes selected from the mature eye, gill and symbiotic light organ (LO) tissues. Significant correlations between data based on NanoString and RNA-Seq expression profiles were observed (Pearson coefficient correlation of 0.7119, $p < 0.0002$), indicating the reliability of RNA-Seq for gene-expression analyses. In bold, genes co-validated with RT-qPCR. **B.** Comparison of log_2-fold change values of transcripts of the same three organs determined by RT-qPCR and NanoString Technologies. (Pearson coefficient of correlation = 0.992, $p < 0.01$). Genes were either up-regulated (+); or, down-regulated (-) with symbiosis. ANP-CE; atrial natriuretic peptide-converting enzyme; ACE: angiotensin-converting enzyme, BPI3: bactericidal/permeability-increasing protein 3; GAPDH: glyceraldehyde-3-phosphate dehydrogenase; Ester hydrolase: ester hydrolase C11orf54 homolog; EBP: emopamil-binding protein; WD88: WD repeat-containing protein 88. Error bars in the NanoString and RT-qPCR expression data represent 95% CI (Dataset S4).

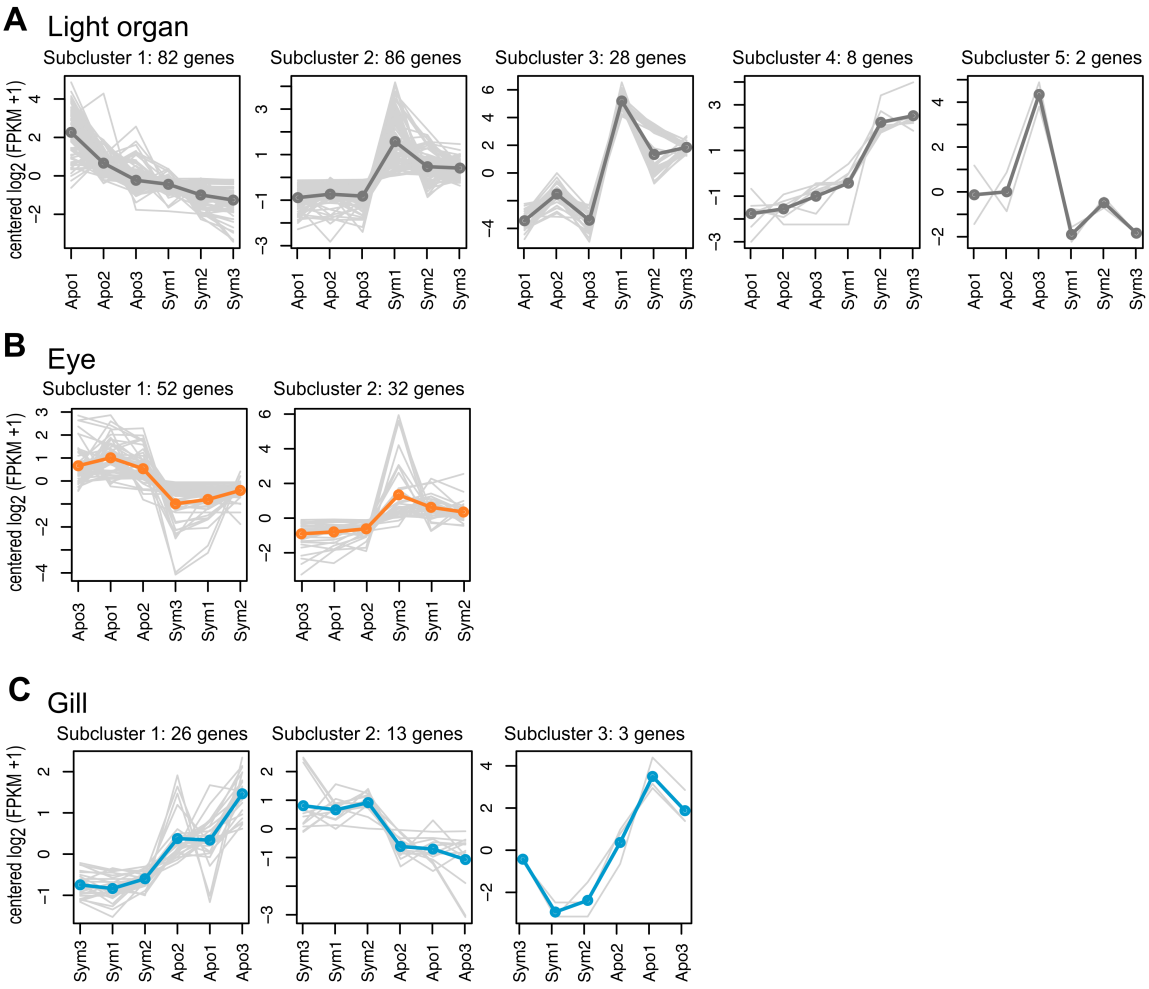

Fig. S5. Patterns of differential gene expression in response to light-organ symbiosis in adult tissues. Differentially expressed genes were grouped into subclusters at 60% of height of the hierarchically clustered gene tree of gene expression. The y-axis gives the median-centered $\log_2$ FPKM, whereas horizontal axes list the different samples. The gray lines represent all mean expression level for all genes in each sub-cluster in **A.** light organ (dark gray); **B.** eye (orange), and **C.** gill (blue). Sym: symbiotic; Apo: aposymbiotic.

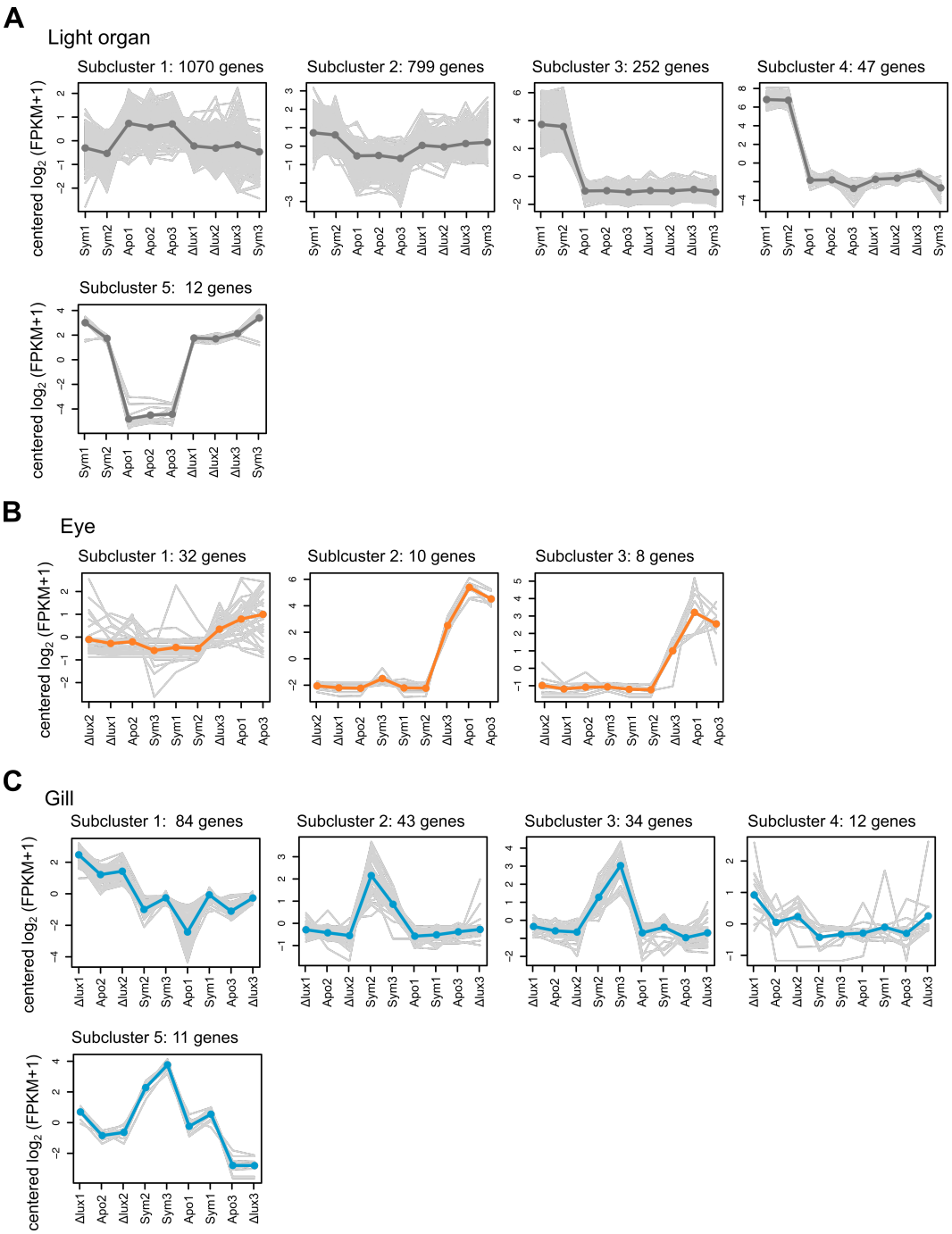

Fig. S6. Patterns of differential gene expression in juvenile tissues in response to light organ symbiosis by luminous and dark bacteria. Differentially expressed genes were grouped into subclusters at 60% of height of the hierarchically clustered gene tree of gene expression. The y-axis gives the median-centered $\log_2$ FPKM, whereas horizontal axes represent the different samples. The light gray lines represent all mean expression level for all genes in each sub-cluster. **A.** light organ (dark gray), **B.** eye (orange), and **C.** gill (blue). Apo (= APO): aposymbiotic; Sym (= SYM): symbiotic, colonized by the wild-type strain ES114; Δlux (= SYM-dark): symbiotic, colonized by the dark mutant Δ*lux* strain EVS102 (4).

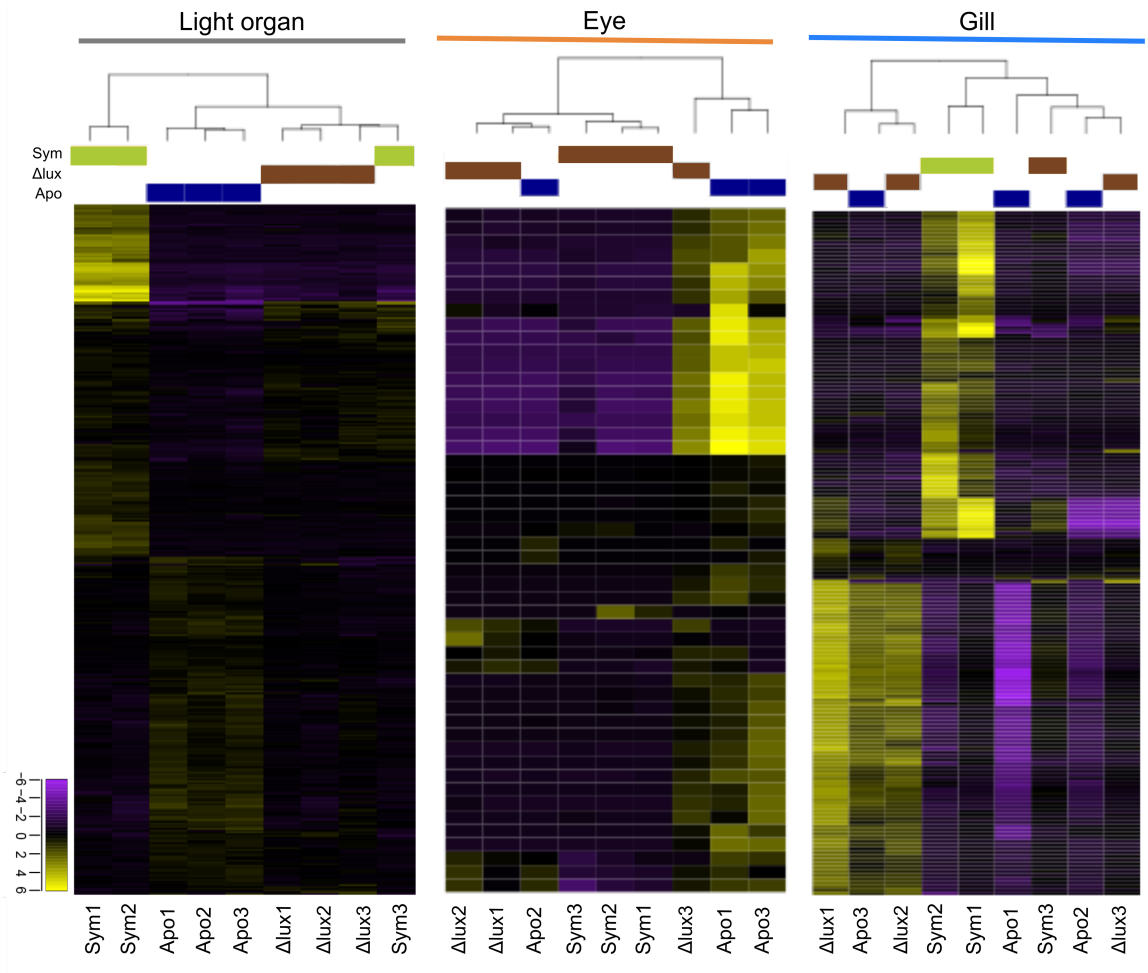

Fig. S7. Transcriptional profiles of juvenile organs in response to light organ colonization by luminous or dark symbionts after 24 h. A heat map of expression values, log_2-transformed and median centered, for genes significantly differentially expressed (>2 fold, P_{adj} <0.05) in juvenile light organ, eye and gill. Apo (= APO): aposymbiotic, (dark blue); Sym (= SYM): symbiotic, colonized with the luminous wild-type strain (in green); Δlux (= SYM-dark): symbiotic, colonized by a dark mutant Δ*lux* strain (in maroon).

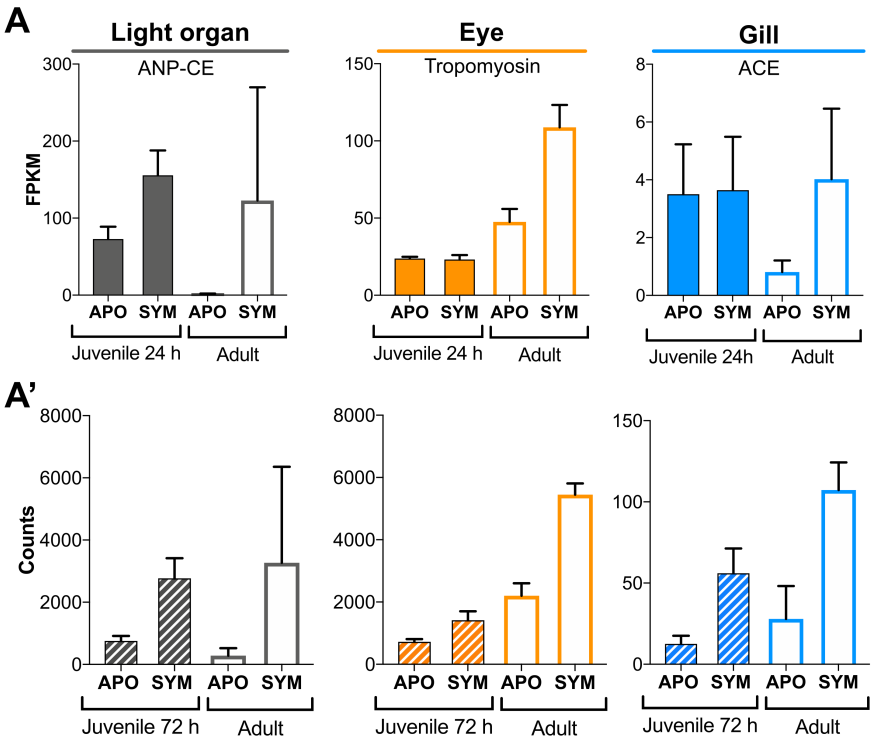

Fig. S8. **Examples of symbiosis-responsive gene expression compared between juvenile and adult organs. A.** Expression of three genes determined by RNA-Seq in 24-h juvenile and in adult animals that had been shown to be differentially regulated in APO and SYM adults, but not in all tissues of 24-h juveniles. **A'.** Expression of the same set of genes determined by NanoString Technologies in 72-h juvenile and in adult animals. APO: aposymbiotic; SYM: symbiotic; ANP-CE: atrial natriuretic-converting enzyme, ACE: angiotensin-converting enzyme.

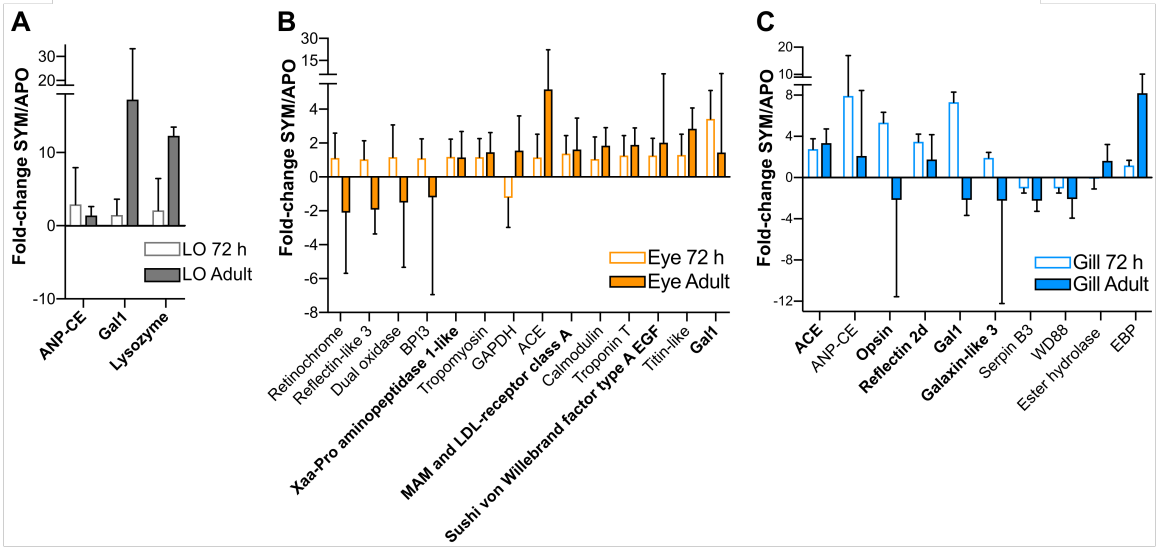

Fig. S9. Differential gene expression early in symbiosis by NanoString Technologies. The $\log_2$-fold change (SYM/APO) values determined by NanoString Technologies, comparing expression values of genes in symbiotic and aposymbiotic squid: light organ (LO) (**A**), eye (**B**) and gill (**C**). ANP-CE; atrial natriuretic peptide-converting enzyme; ACE: angiotensin-converting enzyme. BPI3: bactericidal/permeability-increasing protein 3; GAPDH: glyceraldehyde-3-phosphate dehydrogenase; Ester hydrolase: ester hydrolase C11orf54 homolog; EBP: emopamil-binding protein; WD88: WD repeat-containing protein 88. Error bars indicate one standard deviation. In bold shown 72 h significant fold-changes, *p*-value<0.05 (significance in Dataset S4).

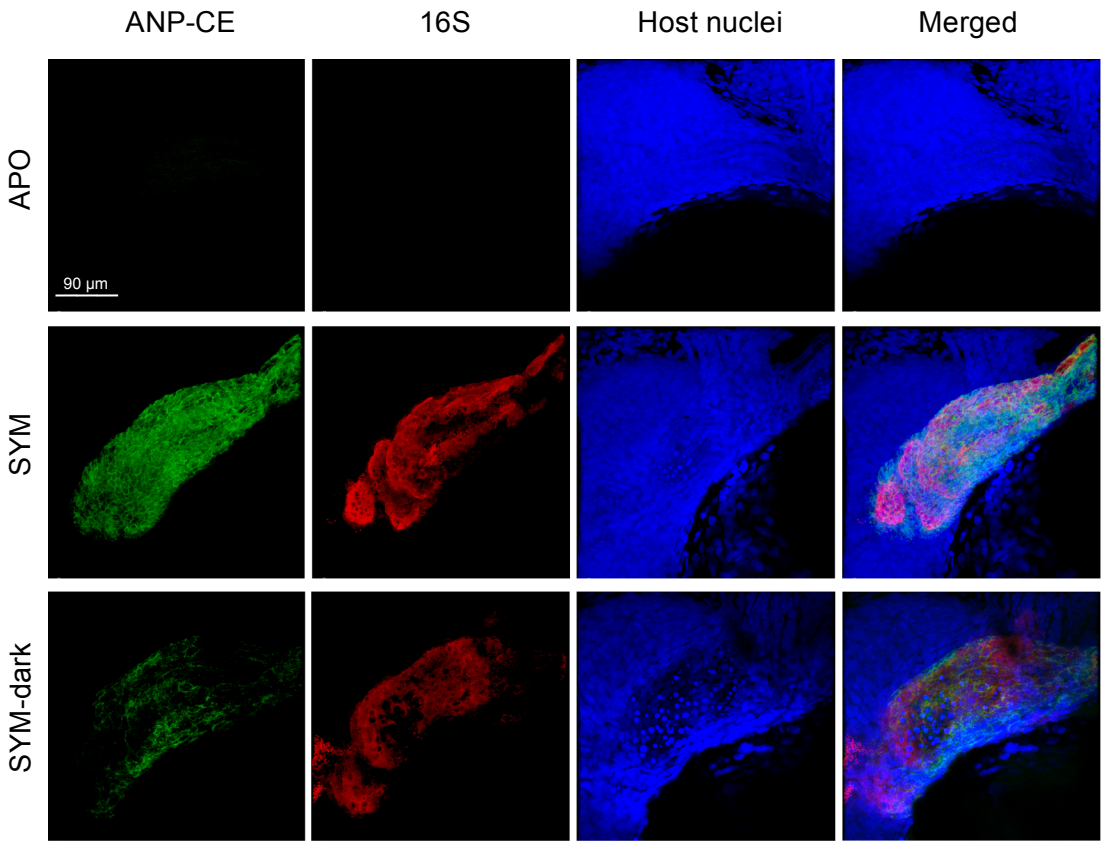

Fig. S10. **Visualization of ANP-CE transcript in whole-mount light organs 24 h after colonization**. Representative confocal images showing ANP-CE expression in crypt epithelium of APO, or SYM or SYM-dark colonized, juvenile squid; merged mid-section of Z-stack of crypt #1. Separate and merged channels: ANP-CE (green), 16S RNA (symbionts, red) and host nuclei (TOPRO, blue) (Movies S1-S3).

326

Table S1. Primer list for RT-qPCR

Gene	*Primer name*	*Primer sequence (5' > 3')*	*Primer reference*
S19 ribosomal protein	40S-qF3 40S-qR3	AAGGCTTTGTCCACCTTCCT TAAATGCTCCAACACCAGCA	This study
Serine hydroxymethyl transferase	HMT-qF HMT-qR	GTCCTGGTGACAAGAGTGCAATGA TTCCAGCAGAAAGGCACGATAGGT	(23)
Heat shock protein 90	HSP90_F HSP90_R	AGACTGCAAGGCTTCCATAAA TTCCGAACAAGGAGGACAATA	This study
Galaxin 1	esgal1_Fq2 esgal1_Rq2	GAACTCGAATCTGTTGTTCTGGCG GTTGGTTTCATGGTAACACGGCCA	(24)
Titin-like	titin_Fq titin_Rq	GCAAAAGTTCTTGGTGCTCA TTGCAACATCTTTGGGCATA	This study
Tropomyosin	tropomy_Fq tropomy_Rq	ATGCTGACCGGAAGTTTGAC GTTGCCCACAACCTTCAACT	This study
Bactericidal/permeability-increasing protein 3	BPI3_Fq BPI3_Rq	GCCAAGTTCGAAATCGTAGC AATCACCAACAACCGCAGTC	This study
Reflectin-like 3	Refl3like_Fq Refl3like_Rq	GACATATCGAAGTATCTTTCTGGGTA GACAGGTGGGGACGTTACTG	This study
Angiotensin-converting enzyme-like isoform X1	ACE_Fq ACE_Rq	AGGTAATATGTGGGCGCAAG CGAAGACGGAGTTTTTCCAG	This study
Galaxin-like isoform X3	galx3_Fq galx3_Rq	ACCCAAACGACAATTCTTGC CAGAGTTTTTCGCTGGTTGA	This study
Opsin	opsin2_Fq opsin2_Rq	GTAAACGGTTTCCCCCTCAT TCTGTGGCTCATATGCTTCG	This study
Reflectin 2d	Ref2d_F Ref2d_R	CAACCCATGTCCCGTATGAC GTCCATCATCCAGCCGTAGT	This study
Atrial natriuretic peptide-converting enzyme	ANPq_F ANPq_R	CATTTCCACCAGCCTTCCTC ATTCGCTTTCGTCCACAACC	This study
WD repeat-containing 88-like	WD88_Fq WD88_Rq	TGAATGGACACATGGATTGG CGAGGGTTGGTCACTTGAAT	This study
Emopamil-binding family-containing	EBP_Fq EBP_Rq	ATGGCAACATGAACGATTCC ATGCAAGAGGGACTGTGTGTC	This study
Ester hydrolase C11orf54 homolog isoform X1	EsterHy_Fq EsterHy_Rq	GGATGCACCTTTGATCTGCT GGCTCGGTATGACACTTCGT	This study
Serpin B3-like isoform X1	serpinB3_Fq serpinB3_Rq	AGCCAGACAACTGGAAGAGGT ATGCGGCTGACTGATTTGA	This study

Table S2. HCR-FISH probe sequences

Probe	Amplifier/Fluorophore	Probe sequence
E. scolopes-ANP-CE #1	B1 / Alexa 488	GCTTGCCTTTATCAAACCTGGACAAAAAATATTTCCCTGCATAGAGTCCGAC
E. scolopes-ANP-CE #2	B1 / Alexa 488	AACAGCTGTGCCCCGACAGTCTTTCCCTTGGCGACAACAGTACGTGCTGGTT
E. scolopes-ANP-CE #3	B1 / Alexa 488	TACCACGGTTGTGGACGAAAGCGAATTGGTGCTCTCCCTTTTGCACTGAGAT
E. scolopes-ANP-CE #4	B1 / Alexa 488	ATCCTAACTCTCTGCAGACAACGTCAGCGTTACTCTGAGACCAATATCCACA
E. scolopes-ANP-CE #5	B1 / Alexa 488	CTGCGGGCTGCATATTGCACGTACACCAAGAGGTGCACTTAGATATGGAGCA
E. scolopes-ANP-CE #6	B1 / Alexa 488	GCTCCTGCGGAATGCATTCATAGTTAAGGCATTGGAATTGGTTCCGATCGCA
E. scolopes-ANP-CE #7	B1 / Alexa 488	AACAATGGAATTCATCGGATCCGCTTTTGCAATTTCTGACGCCATCACATTG
E. scolopes-ANP-CE #8	B1 / Alexa 488	AGATGCCTTTACCGCGATAGACGGATGGACCAACTGAGGCATCTCCTTTTCC
E. scolopes-ANP-CE #9	B1 / Alexa 488	TTTTGTAACCGGGCAATACGGGATTTCTTGCTGCTGCTCCTCTATAGGTAAA
E. scolopes-ANP-CE #10	B1 / Alexa 488	CATCCTGACCGTATAGGATCATGGGATCATACAATTTGGAACTCCGTGTTCC
E. scolopes-ANP-CE #11	B1 / Alexa 488	TACAGTGTGCAGCTGTGAGAACGTGCCATCTGTCAACAATTGCTGCACCACA
E. scolopes-ANP-CE #12	B1 / Alexa 488	CTATCGGCGAAGTCACACGCAATACAGCAATATCGTTGTGCAGTTTCACCTC
E. scolopes-ANP-CE #13	B1 / Alexa 488	GTGGAACCCACGGTTTAGAAGGAAGACATATGGGTCGGATGTAATCAGTCAT
E. scolopes-ANP-CE #14	B1 / Alexa 488	TCGATGTTCGATTATTTTGCATGCGTCCCCAACCCGATAGAAAGCATTGCGT
E. scolopes-ANP-CE #15	B1 / Alexa 488	GACCTCTGCAGCCTTTGTGTCCGAAGCTGACGAGTCCAACTACTTCCCAATA
E. scolopes-ANP-CE #16	B1 / Alexa 488	GGACCCAACTTTTCATTGCATAAACATCGGTAAAGAACAGCGAGTAGTATAC
E. scolopes-ANP-CE #17	B1 / Alexa 488	AGGACCTACCAGCCATTCGTTTTCGGACTGTTGCTTCCCTCCACTTTATTGT
E. scolopes-ANP-CE #18	B1 / Alexa 488	GCAGGAATCTCCTATTTCGGCGGTGGAGTTGTCCGCCTCTTGCATCTACTTC
E. scolopes-ANP-CE #19	B1 / Alexa 488	ATGCGTGTAGTCTGATGTAACCTGAGAACGAGTGTTTTGACTCGGGCGTTTT
E. scolopes-ANP-CE #20	B1 / Alexa 488	GTGCAGGTTTTCGAATAATGCGTCCTGAACGTGTAGTCAGCTGTTGGCTGTC
V. fischeri-16S #1	B3 / Alexa 546	GTTCATTAAGTCAGATGTGAAAGCCCGGGGCTCAACCTCGGAACCGCATTTG
V. fischeri-16S #2	B3 / Alexa 546	ACTGGTGAACTAGAGTGCTGTAGAGGGGGGTAGAATTTCAGGTGTAGCGGTG

Caption for Movie S1. Z-stack of confocal microscopy sections from a representative uncolonized (APO) light-organ crypt #1 (see Fig. 4B, top panel, for single image). The tissue was probed by HCR-FISH to localize symbiont 16S (green) and host ANP-CE (red) RNA, and counterstained to show the epithelial cell nuclei (blue).

Caption for Movie S2. Z-stack of confocal microscopy sections from a representative wild-type *V. fischeri* colonized (SYM) light-organ crypt #1, produced from a Z-stack of confocal microscopy images (see Fig. 4B, middle panel, for single image). The tissue was probed by HCR-FISH to localize symbiont 16S (green) and host ANP-CE (red) RNA, and counterstained to show the epithelial cell nuclei (blue).

Caption for Movie S3. Z-stack of confocal microscopy sections from a representative dark-mutant *V. fischeri* colonized (SYM-dark) light-organ crypt #1, produced from a Z-stack of confocal microscopy images (see Fig. 4B, lower panel, for single image). The tissue was probed by HCR-FISH to localize symbiont 16S (green) and host ANP-CE (red) RNA, and counterstained to show the epithelial cell nuclei (blue).

Dataset S1. *E. scolopes* transcriptome gene expression description. Sheet 1: A description of the raw read counts of the samples sequenced in this study for the *E. scolopes* transcriptome. Sheet 2: Trinity Assembly Statistics. Sheet 3: Top-BLAST hits annotation for the *E. scolopes* transcriptome. Sheet 4: Functional annotation for the *E. scolopes* transcriptome.

Dataset S2. Normalized transcript abundance expressed as FPKM.

Dataset S3. Functional enrichment by tissue type. Sheet 1: GO terms enriched in light organ. Sheet 2: GO terms enriched in eye. Sheet 3: GO terms enriched in gill. Sheet 4: summary of the number of enriched genes by tissue type and number of enriched GO terms. Sheet 5: Enriched GO terms in all juvenile tissues. Sheet 6: Enriched GO terms in all adult tissues.

Dataset S4. Host organ gene-expression data obtained by NanoString Technologies codeset. Sheet 1: NanoString Technologies probe sequences. Sheet 2: 72-h juvenile light-organ expression data. Sheet 3: Adult light-organ expression data. Sheet 4: 72-h juvenile eye expression data. Sheet 5: Adult eye expression data. Sheet 6: 72-h juvenile gill expression data. Sheet 7: Adult gill expression data.

Dataset S5. Transcripts identified as differentially expressed in adult squids by edgeR. Sheet 1, 2: light organ, differently expressed transcripts, raw counts, and annotations. Sheet 3, 4: eye, differently expressed transcripts, raw counts, and annotations. Sheet 5, 6: gill, differently expressed transcripts, raw counts, and annotations.

Dataset S6. Functional enrichment in response to symbiosis. Sheet 1: GO terms enriched in light organ symbiosis-responsive genes. Sheet 2: GO terms enriched in eye symbiosis-responsive genes. Sheet 3: GO terms enriched in gill symbiosis-responsive genes. Sheet 4: Top 5 biological processes enriched within each tissue, as indicated in Fig. 2*C*.

Dataset S7. Transcripts Identified as Differentially Expressed in adult mice eye. Sheet 1: A description of the raw read counts of the samples sequenced in this study for the *M. musculus* eye transcriptome. Sheet 2: Differentially expressed transcripts, raw counts per sample and annotation. Sheet 3: Functional annotation of differentially expressed transcripts.

Dataset S8. Transcripts identified as differentially expressed in juvenile squid by edgeR. Sheet 1, 2: light organ differently expressed transcripts, raw counts, and its annotations in SYM vs APO pairwise comparisons. Sheet 3, 4: light organ differently expressed transcripts, raw counts, and its annotations in SYM-dark (LUX) vs APO pairwise comparisons. Sheet 5, 6: light organ, differently expressed transcripts, raw counts, and its annotations in SYM vs SYM-dark (LUX) pairwise comparisons. Sheet 7, 8: eye, differently expressed transcripts, raw counts, and its annotations in SYM vs APO pairwise comparisons.

Dataset S9. Functional enrichment in response to symbiosis in juvenile squid. Sheet 1: GO terms enriched in juvenile light organ symbiosis-responsive genes. Sheet 2: GO terms enriched in juvenile light organ bioluminescence-specific response. Sheet 3: GO terms enriched in juvenile light organ bacteria-specific response (shared SYM and SYM-dark response). Sheet 4: GO terms enriched in symbiosis-shared response with adult light organ. Sheet 5: GO terms enriched in juvenile eye symbiosis-responsive genes

Dataset S10. Functional gene-set enrichment analysis (GSEA). Sheet 1: Adult light organ GSEA analysis. Sheet 2: Adult eye GSEA analysis. Sheet 3: Adult gill GSEA analysis. Sheet 4: Juvenile light organ GSEA analysis. Sheet 5: Juvenile eye GSEA analysis.

References

1. Naughton LM & Mandel MJ (2012) Colonization of *Euprymna scolopes* squid by *Vibrio fischeri*. *J Vis Exp* (61):e3758.
2. Boettcher KJ & Ruby EG (1990) Depressed light emission by symbiotic *Vibrio fischeri* of the sepiolid squid *Euprymna scolopes*. *J Bacteriol* 172(7):3701-3706.
3. Koch EJ, Miyashiro T, McFall-Ngai MJ, & Ruby EG (2014) Features governing symbiont persistence in the squid-vibrio association. *Mol Ecol* 23(6):1624-1634.
4. Bose JL, Rosenberg CS, & Stabb EV (2008) Effects of *luxCDABEG* induction in *Vibrio fischeri*: enhancement of symbiotic colonization and conditional attenuation of growth in culture. *Arch Microbiol* 190(2):169-183.
5. Graf J, Dunlap PV, & Ruby EG (1994) Effect of transposon-induced motility mutations on colonization of the host light organ by *Vibrio fischeri*. *J Bacteriol* 176(22):6986-6991.
6. Kremer N*, et al.* (2013) Initial symbiont contact orchestrates host-organ-wide transcriptional changes that prime tissue colonization. *Cell Host Microbe* 14(2):183-194.
7. Bolger AM, Lohse M, & Usadel B (2014) Trimmomatic: a flexible trimmer for Illumina sequence data. *Bioinformatics* 30(15):2114-2120.
8. Grabherr MG*, et al.* (2011) Full-length transcriptome assembly from RNA-Seq data without a reference genome. *Nat Biotechnol* 29(7):644-652.
9. Subramanian A*, et al.* (2005) Gene set enrichment analysis: a knowledge-based approach for interpreting genome-wide expression profiles. *Proc Natl Acad Sci U S A* 102(43):15545-15550.
10. Gotz S*, et al.* (2008) High-throughput functional annotation and data mining with the Blast2GO suite. *Nucleic Acids Res* 36(10):3420-3435.
11. Langmead B & Salzberg SL (2012) Fast gapped-read alignment with Bowtie 2. *Nat Methods* 9(4):357-359.
12. Li B & Dewey CN (2011) RSEM: accurate transcript quantification from RNA-Seq data with or without a reference genome. *BMC Bioinformatics* 12:323.
13. Robinson MD, McCarthy DJ, & Smyth GK (2010) edgeR: a Bioconductor package for differential expression analysis of digital gene expression data. *Bioinformatics* 26(1):139-140.
14. de Hoon MJ, Imoto S, Nolan J, & Miyano S (2004) Open source clustering software. *Bioinformatics* 20(9):1453-1454.
15. Vandesompele J*, et al.* (2002) Accurate normalization of real-time quantitative RT-PCR data by geometric averaging of multiple internal control genes. *Genome Biol* 3(7):RESEARCH0034.
16. Untergasser A*, et al.* (2012) Primer3--new capabilities and interfaces. *Nucleic Acids Res* 40(15):e115.
17. Matz MV, Wright RM, & Scott JG (2013) No control genes required: Bayesian analysis of qRT-PCR data. *PLoS One* 8(8):e71448.
18. Kim D & Salzberg SL (2011) TopHat-Fusion: an algorithm for discovery of novel fusion transcripts. *Genome Biol* 12(8):R72.
19. Li H (2011) A statistical framework for SNP calling, mutation discovery, association mapping and population genetical parameter estimation from sequencing data. *Bioinformatics* 27(21):2987-2993.
20. Liao Y, Smyth GK, & Shi W (2014) featureCounts: an efficient general purpose program for assigning sequence reads to genomic features. *Bioinformatics* 30(7):923-930.

21. Nikolakakis K, Lehnert E, McFall-Ngai MJ, & Ruby EG (2015) Use of hybridization chain reaction-fluorescent *in situ* hybridization to track gene expression by both partners during initiation of symbiosis. *Appl Environ Microbiol* 81(14):4728-4735.
22. Schindelin J*, et al.* (2012) Fiji: an open-source platform for biological-image analysis. *Nat Methods* 9(7):676-682.
23. Wier AM*, et al.* (2010) Transcriptional patterns in both host and bacterium underlie a daily rhythm of anatomical and metabolic change in a beneficial symbiosis. *Proc Natl Acad Sci U S A* 107(5):2259-2264.
24. Heath-Heckman EA*, et al.* (2014) Shaping the microenvironment: evidence for the influence of a host galaxin on symbiont acquisition and maintenance in the squid-*Vibrio* symbiosis. *Environ Microbiol* 16(12):3669-3682.